TYPE Original Research PUBLISHED 01 December 2025 DOI 10.3389/feart.2025.1672749



OPEN ACCESS

EDITED BY

Shailesh Kumar Singh National Institute of Water and Atmospheric Research (NIWA), New Zealand

REVIEWED BY

Panayiotis Dimitriadis, National Technical University of Athens, Greece Denis Bwire

Ben-Gurion University of the Negev, Israel

*CORRESPONDENCE

Mark Tuschen.

uschen@uni-bonn.de
 tuschen@uni-bonn.de
 in tuschen
 in tuschen@uni-bonn.de
 in tuschen@uni-bonn.de
 in t

RECEIVED 24 July 2025 REVISED 29 October 2025 ACCEPTED 10 November 2025 PUBLISHED 01 December 2025

CITATION

Tuschen M, Steinbach S, Sin HP and Evers M (2025) Assessing the impact of global change on flood dynamics and rice submergence susceptibility in the Kilombero floodplain, Tanzania

Front. Earth Sci. 13:1672749. doi: 10.3389/feart.2025.1672749

© 2025 Tuschen, Steinbach, Sin and Evers. This is an open-access article distributed under the terms of the Creative Commons Attribution License (CC BY). The use, distribution or reproduction in other forums is permitted, provided the original author(s) and the copyright owner(s) are credited and that the original publication in this journal is cited, in accordance with accepted academic practice. No use, distribution or reproduction is permitted which does not comply with these terms.

Assessing the impact of global change on flood dynamics and rice submergence susceptibility in the Kilombero floodplain, Tanzania

Mark Tuschen^{1*}, Stefanie Steinbach², Hnin Phyu Sin¹ and Mariele Evers¹

¹Department of Geography, University of Bonn, Bonn, Germany, ²Institute of Geography, Ruhr University Bochum, Bochum, Germany

Climate and land use change are increasingly altering the water balance and flood dynamics of East African wetlands. In Tanzania's Kilombero floodplain, rice cultivation relies on seasonal flooding, which is becoming more variable and intense due to climate and land use change. While floodwater is essential for rice cultivation, prolonged submergence poses a threat to yields and regional food security. However, it remains unclear how catchment-scale hydrological changes translate into floodplain-scale flood dynamics and submergence risks for rice crops. To address this, we developed a HEC-RAS 2D hydrodynamic model of the Kilombero floodplain, simulating future flood dynamics under climate change (RCP 4.5 and 8.5) and land use change scenarios. We assessed the susceptibility of rice crops to prolonged submergence by integrating flood model outputs with physiological traits of rice plants. Results show that high-emission scenarios (RCP 8.5) and extensive land conversion to rice cultivation in the floodplain significantly increase areas prone to prolonged rice crop submergence compared to baseline conditions and moderate-emission scenarios (RCP 4.5). Rice plant height was the dominant factor influencing submergence susceptibility. Our findings highlight the importance of integrating hydrodynamic modelling with crop characteristics to inform adaptive rice variety selection and agricultural planning in the context of global change.

Kilombero floodplain, Tanzania, climate change, land use and land cover change, HEC-RAS 2D, hydrodynamic modelling, rice submergence susceptibility

1 Introduction

Climate and land use change alter the water balance of East African wetlands (Notter et al., 2013; Näschen et al., 2018; Gabiri et al., 2019; Näschen et al., 2019b; Näschen et al., 2019a; Gabiri et al., 2020). Despite high spatial variability, studies on the effect of climate change on the water cycle in East Africa widely expect an intensification of hydro-climatic extremes (Shongwe et al., 2011; James et al., 2013; Näschen et al., 2019b; Almazroui et al., 2020; Haile et al., 2020). Additionally, East African wetlands are increasingly used for agricultural production due to their relatively large size, fertile soils, and prolonged periods of soil water availability (Sakané et al., 2011; Behn et al., 2018;

Gabiri et al., 2018). Current developments in East Africa show a shift of upland agricultural production into wetlands to increase food security in the region (Dixon and Wood, 2003; Gabiri et al., 2018). This development is driven by population growth, degradation, and overuse of upland soils and increasing rainfall variability due to climate change (Sakané et al., 2011; Behn et al., 2018; Burghof et al., 2018).

The Kilombero Valley in Tanzania shows evidence of these developments. It contains a floodplain wetland embedded in a mountainous catchment and is drained by the Kilombero River, which forms the most important tributary of the Rufiji River, the largest river system in Tanzania (Wilson et al., 2017). Designated as a protected Ramsar Site since 2002 due to its high biodiversity and ecological importance for residents and downstream regions (Mombo et al., 2011; Munishi and Jewitt, 2019), the Kilombero floodplain faces increasing pressure from climate change and Land Use and Land Cover Change (LULCC) impacts.

Recent studies in the Kilombero Valley expect the catchment to face more pronounced hydrological extremes and intensified seasonality due to climate change and LULCC (Näschen et al., 2019b; Näschen et al., 2019a). These changes affect agricultural management practices in the Kilombero floodplain, where seasonal Land Use and Land Cover (LULC) dynamics are strongly dependent on the depth, duration, and extent of the seasonal flooding of the Kilombero River and its tributaries (Leemhuis et al., 2017; Kirimi et al., 2018).

Rice is the main crop in the Kilombero floodplain (Gebrekidan et al., 2020) and land conversion to rice cropland is the primary driver of LULCC in the Kilombero floodplain (Leemhuis et al., 2017; Näschen et al., 2019a; Thonfeld et al., 2020b). The Kilombero floodplain wetland contributes about 9% of Tanzania's rice production and is therefore highly relevant for the region's food security (United Republic of Tanzania, 2004). While the availability of floodwater in the floodplain is an essential condition for wet-season rice cultivation, unfavourable hydrological conditions such as prolonged crop submergence pose a risk to rice plants (Burghof, 2017; Kwesiga et al., 2020; Grotelüschen, 2021; Ayyad et al., 2022). During prolonged crop submergence, rice plants are submerged in water for several days or even weeks, which impairs gas exchange and photosynthesis, resulting in reduced growth and productivity, as well as crop loss (Singh et al., 2011; Singh et al., 2017; Michael et al., 2023a).

However, a critical research gap remains in translating catchment-scale water balance modelling findings into river-reach-scale flood dynamics within the Kilombero floodplain. This is underlined in previous studies, which highlight the need for a hydrodynamic model of the Kilombero floodplain to analyse future flood dynamics affected by climate change and LULCC (Leemhuis et al., 2017; Näschen et al., 2019a). Furthermore, Kwesiga et al. (2020) and Grotelüschen (2021) emphasise the risk of changing flood dynamics for sustainable agricultural management in the floodplain. Specifically, prolonged submergence of rice crops during floods is identified as the main cause of rice yield gaps in the Kilombero floodplain (Kwesiga et al., 2020).

Therefore, the main objective of this study is to investigate the occurrence of prolonged rice crop submergence in the Kilombero floodplain under past and future conditions. To achieve this, we simulate spatiotemporal dynamics of seasonal floods under

combined climate change and LULCC scenarios as well as baseline conditions. For this purpose, we establish a HEC-RAS 2D hydrodynamic model for the section of the Kilombero floodplain surrounding the town of Ifakara. We then integrate the output from the hydrodynamic model with selected physiological traits of rice plants from the Kilombero Valley to investigate the susceptibility of rice crops to prolonged submergence. By including the effects of climate change and LULCC on flooding as well as agricultural management practices in the analysis, which we subsume under the term Global Change, this study supports adapted future humanflood interactions.

2 Methods

2.1 Study area

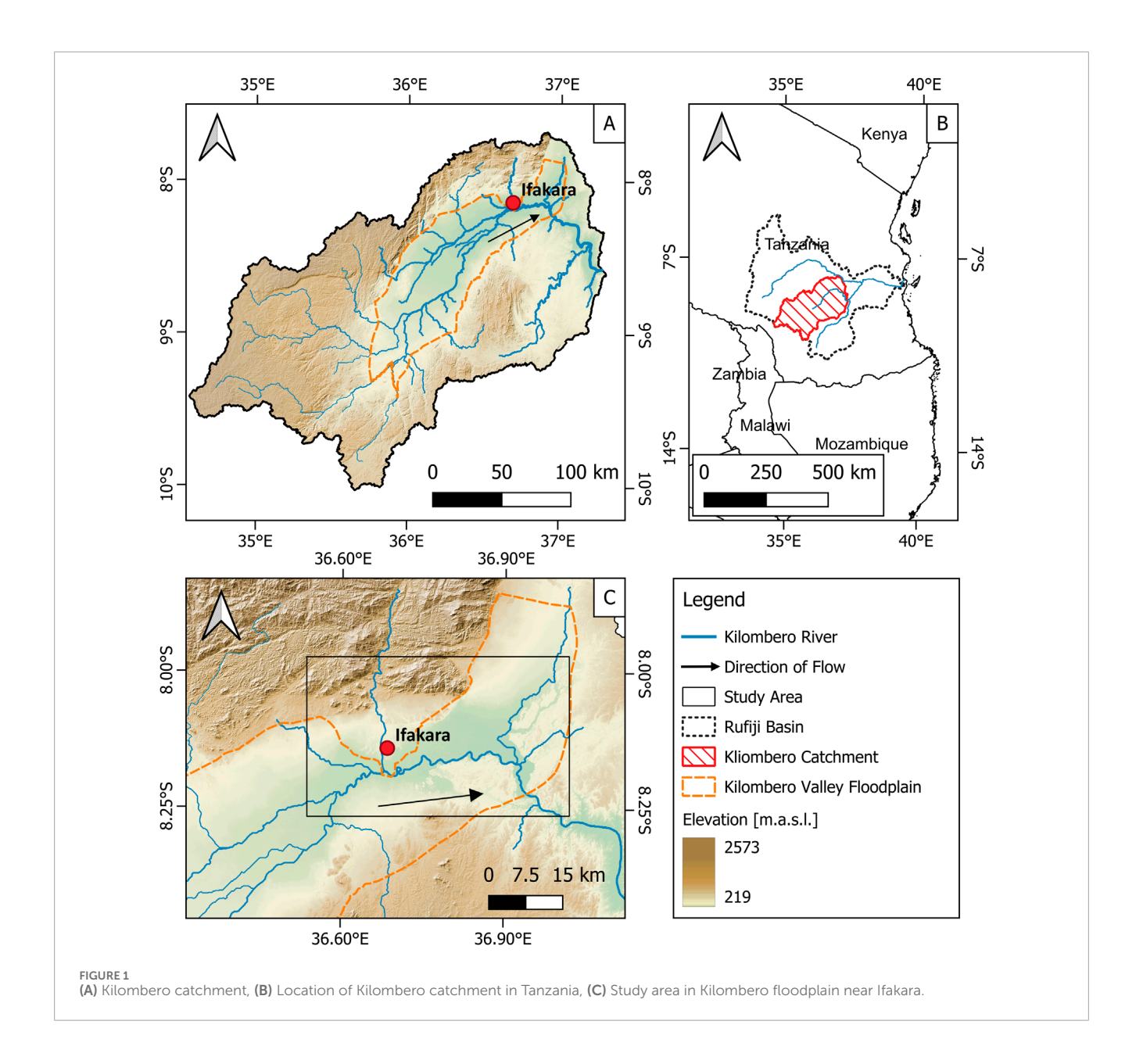
The study area is located around the town of Ifakara within the Kilombero River floodplain in south-central Tanzania, East Africa (see Figure 1). Thus, it is part of the broader Kilombero catchment, which forms one of the four main sub-basins of the Rufiji River Basin and covers an area of approximately 40.000 km² (Mombo et al., 2011; Lyon et al., 2015). The Kilombero River system traverses the flat valley floor and floodplain in a bifurcating and meandering form, following a southwest-to-northeast direction (Jätzold and Baum, 1968). After passing through the town of Ifakara in the northeastern part of the catchment, the river enters a bottleneck-like terrain feature, where the valley floor narrows. An alluvial fan, on which Ifakara is located, acts as a natural dam that retains water during flood season. Water levels can rise to 4.5 m over the riverbanks at this location (Daconto et al., 2018; Kirimi et al., 2018).

Past this point, the river turns in a NW-SE direction, flowing into the Rufiji River, which ultimately drains into the Indian Ocean near Dar es Salaam (Kato, 2007). The climate in the Kilombero catchment is sub-humid tropical (Koutsouris et al., 2016). A distinct spatiotemporal variability characterises the precipitation within the catchment area. The mountains and low-altitude southwest plains receive between 1,500-2,100 mm of annual rainfall, while most lowlands receive only 1,200-1,400 mm annually (Wilson et al., 2017). Distinct rainy and dry seasons are observable. The rainy season roughly spans from November to April, and the dry season from June to October. However, the rainy season exhibits a bimodal pattern and can be subdivided into the short rains (November-January) and the long rains (March-May) (Koutsouris et al., 2016; Wilson et al., 2017). The climate leads to seasonal flooding of the Kilombero floodplain, mainly during the wet season from December to May, while from June to November, it dries up (Munishi and Jewitt, 2019).

2.2 Data

The input data for a HEC-RAS 2D hydrodynamic model comprises river discharge data, surface roughness data, terrain data, and satellite imagery of flood extent, which are used to validate the model (see Table 1).

We obtained discharge input data for the upper boundary condition of the hydrodynamic model and four tributaries from



the hydrological Soil and Water Assessment Tool (SWAT) model of the Kilombero catchment set up by Näschen et al. (2019a). Further details about the model calibration, validation, and scenarios are provided by Näschen et al. (2019a) and Näschen et al. (2018). The authors provided discharge hydrographs with daily values for the 2050-2060 period under two Representative Concentration Pathways (RCP). Both RCP scenarios were available with a specific Global Climate Model (GCM) - Regional Climate Model (RCM) combination. Namely, RCP 4.5 with GCM: CNRM-CM5 and RCM: CCLM4-8-17_v1 and RCP 8.5 with GCM: MIROC5 and RCM: RCA4_v1 (see Table 1). RCP 4.5 assumes moderate greenhouse gas emissions and a radiative forcing of 4.5 W m-2, while RCP 8.5 assumes very high greenhouse gas emissions without efforts to constrain and a radiative forcing of 8.5 W m-2 at the end of the twenty-first century (Collins et al., 2013; Näschen et al., 2019b). The GCM-RCM combinations represent a range of wet and dry scenarios covering increasing and decreasing annual precipitation amounts compared to historical data (1951–2005) (Näschen et al., 2019a). For RCP 4.5, the driest available GCM-RCM combination was chosen (–8.3% annual precipitation compared to the past) and for RCP 8.5, the wettest (+22.5% annual precipitation compared to the past).

As a baseline scenario, Näschen et al. (2019a) provided modelled daily discharge values for the 1958–2005 period. Modelled discharge data was used for the baseline scenario due to the lack of measured historical discharge data at the upper boundary of the hydrodynamic model. To produce this data, the SWAT model was run with an Ensemble Mean (EM) of six different historical Cordex RCMs for the 1958–2005 period (Näschen et al., 2019b). Further information about the ensemble members can be found in Näschen et al. (2019b). Additionally, to validate the hydrodynamic model, we retrieved modelled discharge data with daily values from 1 January 2014, to 31 December 2014, from the SWAT model to

TABLE 1 Overview of the used datasets, their resolution, timeframe, conditions, source, and purpose.

Data set	Resolution/Timeframe/Conditions	Source	Purpose
Discharge	Daily/2050–2060/RCP 4.5 and RCP 8.5 Daily/2014/RCP 8.5 Daily/1958–2005/CORDEX historical ensemble mean	Näschen et al. (2019a)	Input hydrographs HEC-RAS model
LULC	90 m/1994/historical 30 m/2014/historical 90 m/2030/LULCC Extreme 30 m/2030/LULCC Business as usual 30 m/2030/LULCC Conservation	Thonfeld et al. (2020b) Thonfeld et al. (2020b) Proswitz et al. (2021) Proswitz et al. (2021) Proswitz et al. (2021)	Surface roughness HEC-RAS model
Copernicus GLO-30 DEM	30 m/2011–2015	European space agency (ESA)	Terrain HEC-RAS model
Satellite images	30 m/10.05.2014 & 11.05.2014	USGS earth explorer	Validation

compare the modelled maximum flood extent for that year with the observed maximum flood extent. The 2014 discharge data were extracted under RCP 8.5 conditions (the wettest GCM-RCM combination), as historical RCM data ended in 2005, and there was no available measured discharge data for 2014 at the upper boundary condition and the tributaries of the hydrodynamic model. RCP 8.5 was chosen over RCP 4.5 to align with the severity of the 2014 flood (Kirimi et al., 2018).

We obtained Manning's n surface roughness coefficients for each land use class from the Natural Resources Conservation Center (NRCS) of the United States Department of Agriculture (USDA) (Janssen, 2016) and Emery et al. (2021) (see Table 2). We gathered five different LULC scenarios for the study area: 1994 and 2014 LULC data by Thonfeld et al. (2020b) and three LULCC projections for 2030 by Näschen et al. (2019a) and Proswitz et al. (2021) (see Table 1). The 1994 LULC classification was used for a baseline scenario, whereas the 2014 classification was used for a model validation scenario. Näschen et al. (2019a) provided a projection of LULCC for 2030 with an extreme level of conversion of natural land to (rice) cropland, from here on named LULCC Extreme (Näschen et al., 2019a). Proswitz et al. (2021) provided a Businessas-usual (BAU) and a Conservation LULCC projection for 2030, from here on named LULCC BAU and LULCC Conservation. The LULCC BAU scenario assumes that existing trends and policy decisions, as well as the intensification and expansion of agricultural land, will continue without interventions. The LULCC Conservation scenario assumes that protected areas are effectively managed and protected, and no further land is to be converted into cropland where prohibited (see Table 2). Detailed information on methodologies and underlying assumptions can be found in the respective publications.

We used the COPERNICUS GLO-30 digital elevation model (DEM) by the European Space Agency (ESA) as terrain input data (see Table 1). The 30 m spatial resolution DEM has already been processed for hydrological applications. It is based on the 12 m TanDEM-X DEM by the German Aerospace Center (DLR), which was acquired between 2011 and 2015 and underwent terrain editing (including water body flattening) (Airbus, 2022; ESA, 2025).

For model validation, the maximum flood extent of the 2014 flood event in the Kilombero floodplain was derived from satellite images and compared with model results. We downloaded Landsat images pre-processed to surface reflectance from the United States Geological Survey (USGS) Earth Explorer (see Table 1). The Landsat 8 Operational Land Imager (OLI) image from 10/05/2014 (path 168, row 66) and the Landsat 7 Enhanced Thematic Mapper Plus (ETM+) from 11/05/2014 (path 167, row 66) showed the largest flood extent for this rainy season. We performed cloud masking using the function of mask (Fmask) stored in the pixel quality files (Zhu and Woodcock, 2012; Zhu et al., 2015). We then calculated the Normalized Difference Vegetation Index (NDVI) (Tucker, 1979) and the Normalized Difference Water Index (NDWI) (McFeeters, 1996), appended them to the individual image stacks and mosaicked the images. We carried out a Random Forest (RF) supervised classification to derive a water mask. RF is widely used for land cover classification, including wetland monitoring (Corcoran et al., 2015; Millard and Richardson, 2015; Gxokwe et al., 2022), and specifically in the Kilombero catchment (Thonfeld et al., 2020a). As training data, we created a set of 300 random samples for water and

TABLE 2 Share of LULC classes in LULC scenarios within the model domain and Manning's n roughness coefficients.

LULC class	Manning's n roughness coefficient (source)	1994	2014	2030 extreme	2030 BAU	2030 conservation
Built-up	0.1 (USDA)	0.03%	0.1%	0.1%	0.1%	0.1%
Closed woodland	0.16 (USDA)	11.8%	11.9%	12%	11.9%	11.8%
Cropland	0.035 (USDA)	17.7%	18.3%	8%	19.2%	18.3%
Grassland	0.035 (USDA)	34.2%	24.9%	9.5%	17.4%	24.6%
Montane Forest	0.16 (USDA)	0%	0%	0%	0%	0%
Savanna	0.03 (USDA)	31.7%	14.3%	13.3%	12.2%	14%
Rice	0.083 (according to Emery et al. (2021))	1.2%	28.6%	55.3%	37.4%	29.3%
Swamp	0.07 (USDA)	1.7%	0.2%	0.2%	0.2%	0.2%
Water (main channel)	0.04 (USDA)	1.6%	1.6%	1.6%	1.6%	1.6%
Teak plantation	0.16 (USDA)	0%	0.01%	0%	0.01%	0.01%

400 for non-water classes in the catchment and visually interpreted them based on the image mosaic, which we applied in the EnMap Box software (van der Linden et al., 2015). We further created a valid pixel mask for all observations unaffected by cloud or scan line gaps to restrict the accuracy assessment to these areas.

2.3 Hydrodynamic modelling approach

We ran flood simulations in the Kilombero floodplain using the HEC-RAS 2D hydrodynamic model (HEC-RAS 6.3.1). Hydrodynamic models are commonly used tools for flood mapping, hazard and risk assessment, and flood prediction (Afzal et al., 2022; Alipour et al., 2022; Mubialiwo et al., 2022; Yang et al., 2022). Specifically, the HEC-RAS 2D hydrodynamic model software, employed in this study, finds wide application in flood modelling across various fields of research (Rao et al., 2019; Singh et al., 2020; Yalcin, 2020; Afzal et al., 2022; Alipour et al., 2022). In floodplain wetland environments, hydrodynamic models provide valuable information for floodplain management, which can enhance decision-making and planning of climate change adaptation and mitigation measures (Chomba et al., 2021).

There are two common approaches for flood simulation through a hydrodynamic model: one-dimensional (1D) and two-dimensional (2D). 1D models consider only the longitudinal flow for the main channel and floodplains. 2D models, on the other hand, consider longitudinal and lateral flow in the main channel and floodplains (Afzal et al., 2022). 1D models are quicker to create, while 2D models have a finer spatial and temporal resolution but are associated with higher computational costs (Timbadiya et al., 2011; Yang et al., 2022). HEC-RAS 2D has demonstrated reliable performance for flood estimation (Pinos

and Timbe, 2019) and has been successfully applied in studies in East Africa (Desalegn and Mulu, 2021; Mubialiwo et al., 2022) as well as in wetland modelling studies (Alawadi et al., 2023). Hydrodynamic modelling to investigate growing conditions for rice has been successfully conducted in South Africa by Kleynhans et al. (2007) and in India by Samantaray et al. (2015), supporting our approach.

2D hydrodynamic models, such as HEC-RAS 2D, simulate the spatiotemporal propagation of water through a given area by solving physics-based equations (Yang et al., 2022). The HEC-RAS 2D model performs flood simulations by solving 2D Saint-Venant diffusive wave equations using the numerical finite-volume method (Brunner, 2021; Afzal et al., 2022; Mubialiwo et al., 2022). In this study, we applied it to compute the maximum flood depths per pixel, the flood depth per pixel over time, and the flood extent over time.

The HEC-RAS 2D model was set up with the COPERNICUS GLO-30 DEM as terrain input, Manning's n roughness coefficients attributed to LULC data, 365-day discharge hydrographs as the inputs for the upper boundary condition and four tributaries, and a normal depth configuration as the lower boundary condition of the model. Normal depth was chosen for the lower boundary condition of the model due to the lack of measured or modelled discharge hydrographs and rating curves for this point on the Kilombero River. With the normal depth configuration, HEC-RAS can back-calculate water stage at the lower boundary from Manning's Equation using the friction slope, flow, Manning's n value, and the cross-section shape (Brunner, 2021). According to the HEC-RAS manual, we used the local bed slope (0.0002) as the friction slope. To initiate the model runs, we set initial conditions to ramp up the water surface in the model over 48 h to achieve a continuous water surface in the Kilombero River before the model run (Brunner, 2021). The computational timestep of the model was set to 1 h, while the output

TABLE 3 Input scenarios of the hydrodynamic model with discharge (including climate change signal) input and LULC(C) input signals.

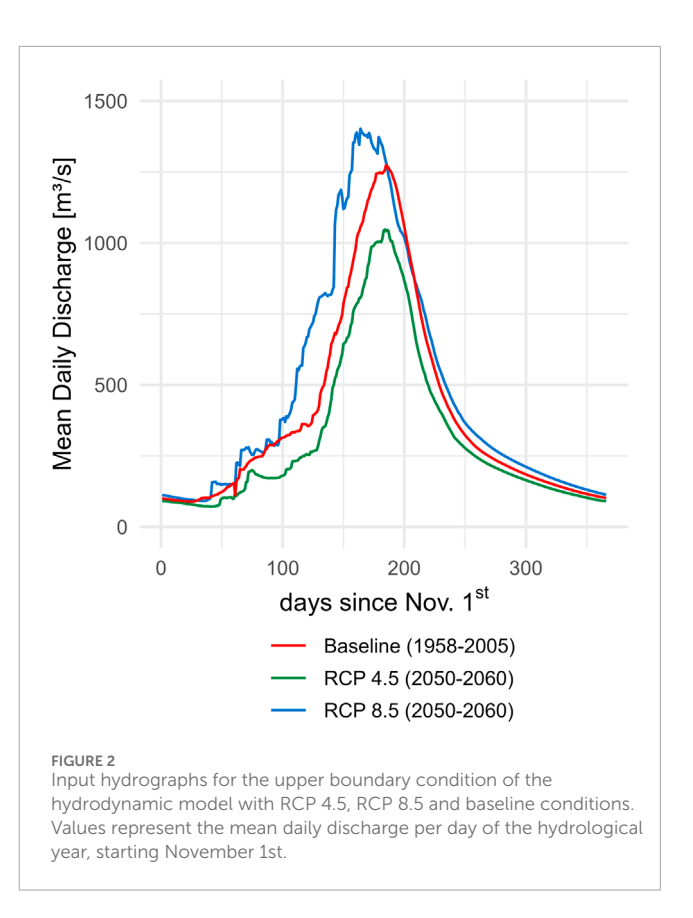
Flood scenario	Discharge/Timespan	LULC(C)	
A	RCP 8.5 2050-2060	2030 extreme	
В	RCP 4.5 2050-2060	2030 extreme	
С	RCP 8.5 2050-2060	2030 BAU	
D	RCP 4.5 2050-2060	2030 BAU	
Е	RCP 8.5 2050-2060	2030 conservation	
F	RCP 4.5 2050-2060	2030 conservation	
Validation	RCP 8.5 2014	2014	
Baseline	Cordex hist. Ensemble mean 1958–2005	1994	

interval was set to 1 day (see Supplementary Table S1). The intervals were determined through an iterative process aimed at achieving the best possible temporal resolution while keeping computation time within reasonable limits and avoiding model instability. The start and end dates were set to November 1st to simulate a full hydrological year.

The model domain covers a size of $871.3 \,\mathrm{km^2}$ and a river reach length of $60.5 \,\mathrm{km}$. Within the domain, the cell size of the computational mesh was set to $60 \times 60 \,\mathrm{m}$ in an iterative process, which allowed the best possible spatial resolution while keeping the computation time within a reasonable limit and avoiding model instabilities. The stream was covered with a refined mesh of $10 \times 10 \,\mathrm{m}$ cells (see Supplementary Table S1). Cell faces were aligned with the riverbanks and lines of substantial topographical change within the floodplain to avoid premature spill over.

We developed model scenarios by combining hydrological and LULCC input data in different variations (see Table 3). The hydrological input data were prepared by calculating the mean daily discharge for each day of the hydrological year, forming 365-day discharge hydrographs representing the 2050–2060 decade under RCP 4.5 and RCP 8.5 conditions, as well as the 1958–2005 timeframe under baseline conditions (see Figure 2). Input hydrographs were created for the upper boundary condition and four tributaries of the Kilombero River within the model domain. We chose the hydrological year, starting on November 1st, to align with both the wet season and the cropping season, which typically commence around November. Surface roughness data was prepared by linking LULC classes to the respective Manning's n value for each scenario in HEC-RAS.

To validate the hydrodynamic model, we used a scenario mirroring the 2014 flood conditions, which extended up to 3 km on both sides of the river during the rainy season (Kirimi et al., 2018). The model validation incorporated the 2014 LULC dataset as input for surface roughness and the 2014 discharge hydrograph under RCP 8.5 conditions. Observed and modelled maximum flood extent were compared using a contingency table. The table includes True Positives (TP, pixels are flooded in both observed and modelled



data), True Negatives (TN, pixels are dry in observed and modelled data), False Positives (FP, pixels are flooded in the modelled data but not in the observation), and False Negatives (FN, pixels are flooded in the observed data but not in the modelled data). Based on the table, skill scores quantifying the model accuracy were calculated, including Overall Accuracy (OA), Probability of Detection (POD), False Alarm Ratio (FAR), and Critical Success Index (CSI). The OA, POD, FAR, and CSI were calculated using Equations 1–4 (Ming et al., 2025; Thiemig et al., 2015):

$$OA = \frac{TP + TN}{TP + FP + FN + TN} * 100 \tag{1}$$

$$POD = \frac{TP}{TP + FN} * 100 \tag{2}$$

$$FAR = \frac{FP}{TP + FP} * 100 \tag{3}$$

$$CSI = \frac{TP}{TP + FP + FN} * 100 \tag{4}$$

We assessed parameter sensitivity of the model by perturbing the model parameters individually and examining how the model output changed in each case. The tested parameters were discharge, Manning's n, mesh cell size, computational timestep, and slope at the lower boundary condition. Discharge, mesh cell size, and slope were varied by +50%, +20%, 0%, -20%, and -50%. Manning's n was increased by +100% as well. The computational timestep was varied by +100% and -50% due to limitations in the timestep setting options. The results were evaluated in terms of discharge at the lower boundary of the model and flood depth at a central cross-section of the floodplain close to Ifakara (Paiva et al., 2013).

TABLE 4 Scenarios for assessing the susceptibility to prolonged submergence for rice plants in the Kilombero floodplain with selected physiological traits of rice plants: Mature growth height and temporal tolerance to submergence.

Rice scenario	Rice variety	Mature growth height (approx.)	Submergence tolerance
Scenario 1	Saro 5	100 cm	7 days
Scenario 2	Saro 5	100 cm	14 days
Scenario 3	Saro 5	100 cm	21 days
Scenario 4	Supa India	130 cm	7 days
Scenario 5	Supa India	130 cm	14 days
Scenario 6	Supa India	130 cm	21 days

2.4 Assessment of the susceptibility of rice crops to prolonged submergence

Floods and prolonged crop submergence are the main physical stressors and causes of yield gaps in lowland rice farming in the Kilombero floodplain (Kwesiga et al., 2020; Michael et al., 2023a). To assess the susceptibility of rice crops to prolonged submergence, we integrated the hydrodynamic model results from scenarios A-F and the baseline scenario with selected physiological traits of rice plants, including plant height and temporal tolerance to submergence.

Farmers typically encounter floods mainly in March, April, and May, when plants have usually matured (Michael et al., 2023a). Therefore, we assumed mature rice plants for the analysis. The growth height of mature rice plants in the Kilombero floodplain varies with rice variety, site, management practices and other variables (Kitilu et al., 2019). In this study, we adopted the rice plant height values reported by Kitilu et al. (2019), which were measured in field experiments conducted on two different sites near Ifakara and thus reflect natural plant height variability. We chose the tallestgrowing local variety, Supa India (approximately 130 cm), and Saro 5, a relatively short-growing (approximately 100 cm) modified, high-yielding variety (Kitilu et al., 2019; Michael et al., 2023a). Varieties without specific tolerance traits cannot survive more than a week of complete submergence (Xu et al., 2006). Submergenceor flood-tolerant rice varieties (e.g., with the Sub1 gene) can survive fully submerged for 10-14 days and resume growth after the water recedes (Xu et al., 2006; Singh et al., 2017). Examples of highly tolerant varieties can survive complete submergence for up to 21 days (Panda et al., 2021). These values are based on experimental observations and therefore represent approximate ranges that are subject to field variability. Based on the gathered information, we developed six scenarios with different combinations of mature growth height and submergence tolerance to compare these exemplified plant requirements with the hydrodynamic model results (see Table 4).

To quantify the susceptibility of rice crops to prolonged submergence under global change scenarios, we applied a rolling window algorithm to the flood depth per pixel over time output from the hydrodynamic model (scenarios A-F and baseline), using the parameter combinations in the rice scenarios (scenarios 1–6). For each pixel, the algorithm checks whether there exists any stretch

of *y* consecutive days where the depth exceeds *x*. This way, the algorithm returns a binary susceptibility map of the floodplain for each combined scenario, indicating areas where rice plants would be susceptible (1) to prolonged submergence or not (0). This resulted in 42 susceptibility scenario maps (seven flood scenarios multiplied by six rice scenarios).

To examine the relative influence of each input variable (Discharge and LULCC in the hydrodynamic model; rice growth height and rice submergence tolerance as rice plant variables) on the size of the area susceptible to prolonged rice crop submergence, we derived Feature Importance with an RF regression model. Feature Importance analysis is a technique used in machine learning and data analysis to identify and quantify the influence of individual features (variables) on the output of a model (Cappelli and Grimaldi, 2023). For this purpose, the dataset was split into training and testing sets and trained using the scikit-learn machine learning library in Python. R² and Root Mean Squared Error (RMSE) served as performance metric for model fit. To ensure robust validation, we used 5-fold cross-validation and reported the mean R² and RMSE across folds. Feature Importance scores were extracted from the trained model to identify which features contribute the most to the size of the susceptible area.

3 Results

3.1 Hydrodynamic model validation and sensitivity analysis

Model validation was conducted using a contingency table, in which the modelled and satellite-based observed maximum flood extents were compared. Since areas with clouds and scan line gaps were masked from the satellite data, a coverage of 43.5% of the model domain remained. The modelled 2014 maximum flood extent matched the observed maximum flood extent of the same year, with an Overall Accuracy of 91.82% and Probability of Detection of 90.33%. Slight overestimations are visible at elevated areas in the centre of the floodplain, underestimations towards the northern edges of the flooded area. The False Alarm Ratio is 6.64% and the Critical Success Index is 84.88% (see Figure 3; Table 5). The sensitivity analysis revealed that the discharge input at the upper boundary has a significant impact on both the flood depth at the

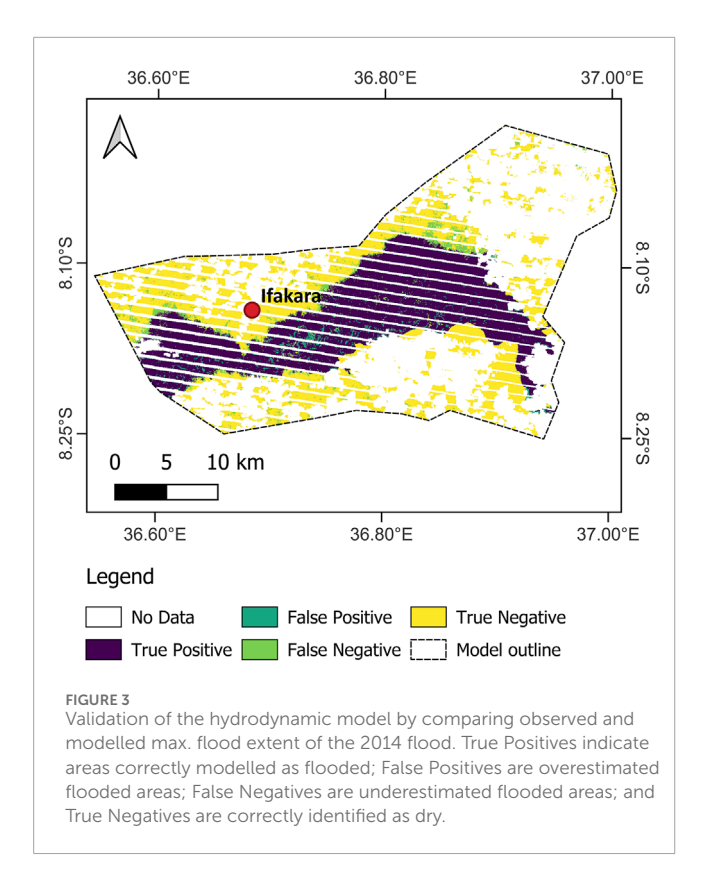


TABLE 5 Contigency table comparing the modelled and observed maximum flood extent in 2014 in the Kilombero floodplain. Yes and no indicate if a pixel was flooded in the respective dataset. Numbers indicate the number of pixels that are either True Positive (TP), False Negative (FN), False Positive (FP), or True Negative (TN).

		Observed			
		Yes	No		
Modelled	Yes	TP: 193125	FP: 13725		
	No	FN: 20675	TN: 192928		

central floodplain cross-section and discharge at the lower model boundary (see Figure 4). Changing the computational mesh cell size had no effect on the discharge at the lower boundary of the model, but did affect the flood depth in the rising and falling limbs of the depth hydrograph. Reducing the cell size led to a flattening of the depth hydrograph, while increasing the cell size led to a steeper hydrograph. Additionally, decreasing cell size negatively affected stability and computation time (e.g., reducing the cell size by -50% increased the computation time by ca. 452%). Perturbing Manning's n roughness coefficient minimally affected discharge at the lower boundary but significantly influenced flood depth. Substantial changes in the discharge hydrograph at the lower boundary start to become more visible with a change in Manning's n of +100%. Slope at the lower boundary condition and computational timestep showed negligible sensitivity. However, reducing the timestep by 50% increased computation time by ca. 300%.

3.2 Flood dynamics in the Kilombero floodplain

With the hydrodynamic model, we simulated spatiotemporal dynamics of the seasonal flood in the Kilombero floodplain under combined climate change and LULCC scenarios (2050-2060) and under baseline conditions (1958-2005) (see Table 1). The primary output variables of the HEC-RAS 2D model employed in this study are the maximum flood depth per pixel, flood depth per pixel over time, and flood extent over time. Analysis of maximum flood depth per pixel in the study area revealed that RCP 8.5 scenarios (A, C, E) yielded higher maximum flood depths compared to the baseline and the RCP 4.5 scenarios (B, D, F) (see Figure 5). The effect of LULCC is evident in the increase in maximum flood depth per pixel from LULCC Conservation to LULCC BAU to LULCC Extreme. The increase is most pronounced in scenarios with LULCC Extreme input signal (A and B). Scenario A shows an increase of 23.1% compared to baseline, whereas scenarios C and E show an increase of 8.8% and 6.6% respectively. Remarkably, the effect of the LULCC signal in scenario B (LULCC Extreme) leads to an increase of maximum flood depth compared to baseline condition (4.4%). In contrast, scenarios D and F (both with an RCP 4.5 input signal) show decreases of -5.5% and -6.6%, respectively.

Flood extent over time showed a similar dynamic to the maximum flood depth per pixel. Scenarios A, C, and E with RCP 8.5 input signal and scenario B with RCP 4.5 and LULCC Extreme input signals show an increase in peak flood extent compared to baseline conditions (see Figure 6). Unlike scenario B (RCP 4.5 and LULCC Extreme), where only the peak flood extent exceeds the baseline, RCP 8.5 scenarios show larger flood extents already during the rising limb of the flood. Scenarios D and F show a smaller flood extent compared to the baseline scenario at all times of the simulation. It is noticeable that the peak flood extent of RCP 8.5 scenarios occurs around day 167, whereas the peak of RCP 4.5 scenarios and the baseline scenario occur around day 187 of the simulation. This corresponds to a peak flood extent in mid-April for RCP 8.5 scenarios, and in early May for RCP 4.5 scenarios and the baseline scenario.

3.3 Susceptibility of rice crops to prolonged submergence in the Kilombero floodplain

Finally, we integrated the hydrodynamic model output with selected physiological traits of rice plants to assess their susceptibility to prolonged submergence. Overall, flood scenarios with wetter climate and more extensive LULCC towards rice cultivation in the floodplain and rice scenarios with short-growing varieties result in larger areas susceptible to prolonged rice crop submergence. The size of the areas decreases with a drier climate input signal and less land use change towards rice cultivation in the flood scenarios, as well as taller varieties in the rice scenarios (see Figure 7). The riparian zone (areas proximal to the Kilombero River) is susceptible to prolonged rice crop submergence in all scenarios. In contrast, the fringe zone (areas distal from the Kilombero River) and middle zone become increasingly susceptible as the scenario becomes more extreme (see Figure 7).

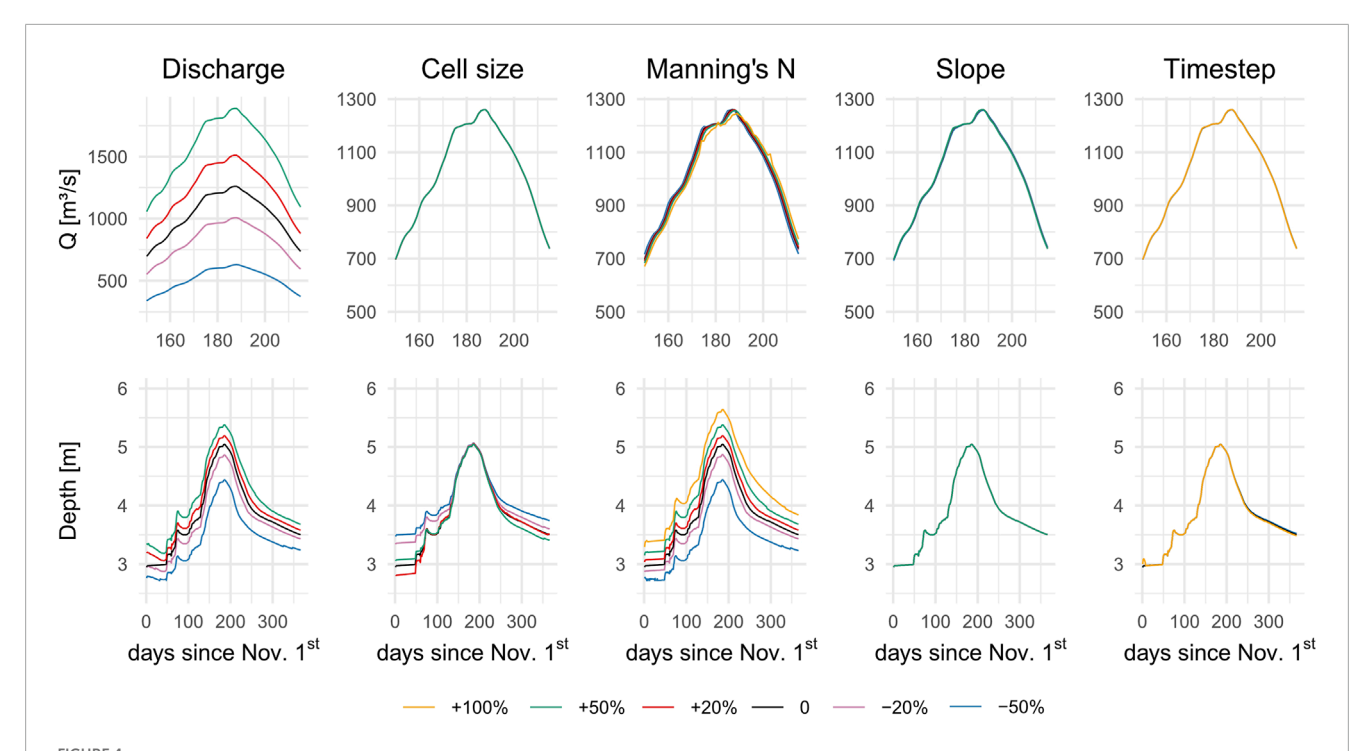


FIGURE 4 Sensitivity analysis: Discharge (Q [m³/s]) at lower model boundary and flood depth [m] at central floodplain cross-section close to Ifakara. Derived from model runs using perturbed values of discharge, mesh cell size, slope at the lower boundary condition and computational timestep. Discharge hydrographs are zoomed in on the period of peak flow.

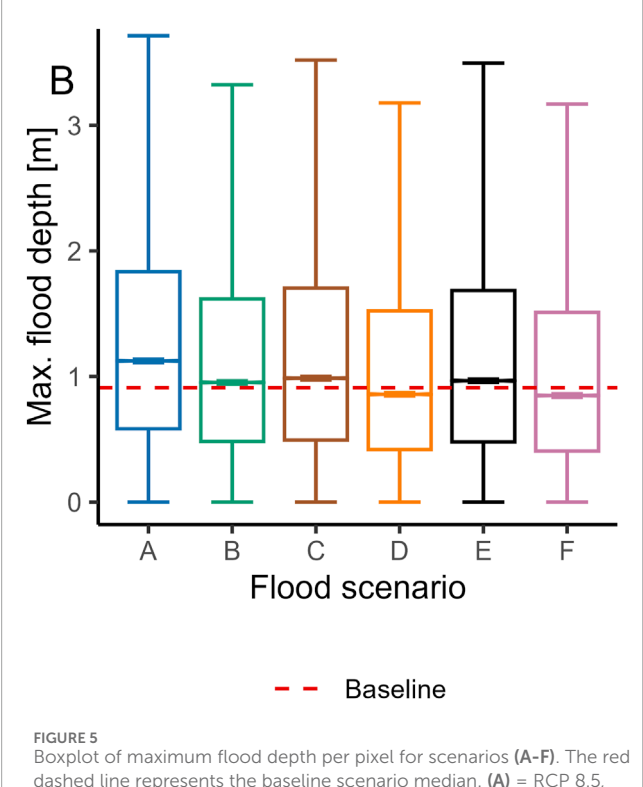


FIGURE 5 Boxplot of maximum flood depth per pixel for scenarios (A-F). The red dashed line represents the baseline scenario median. (A) = RCP 8.5, Extreme; (B) = RCP 4.5, Extreme; (C) = RCP 8.5, BAU; (D) = RCP 4.5, BAU; (E) = RCP 8.5, Conservation; (F) = RCP 4.5, Conservation.

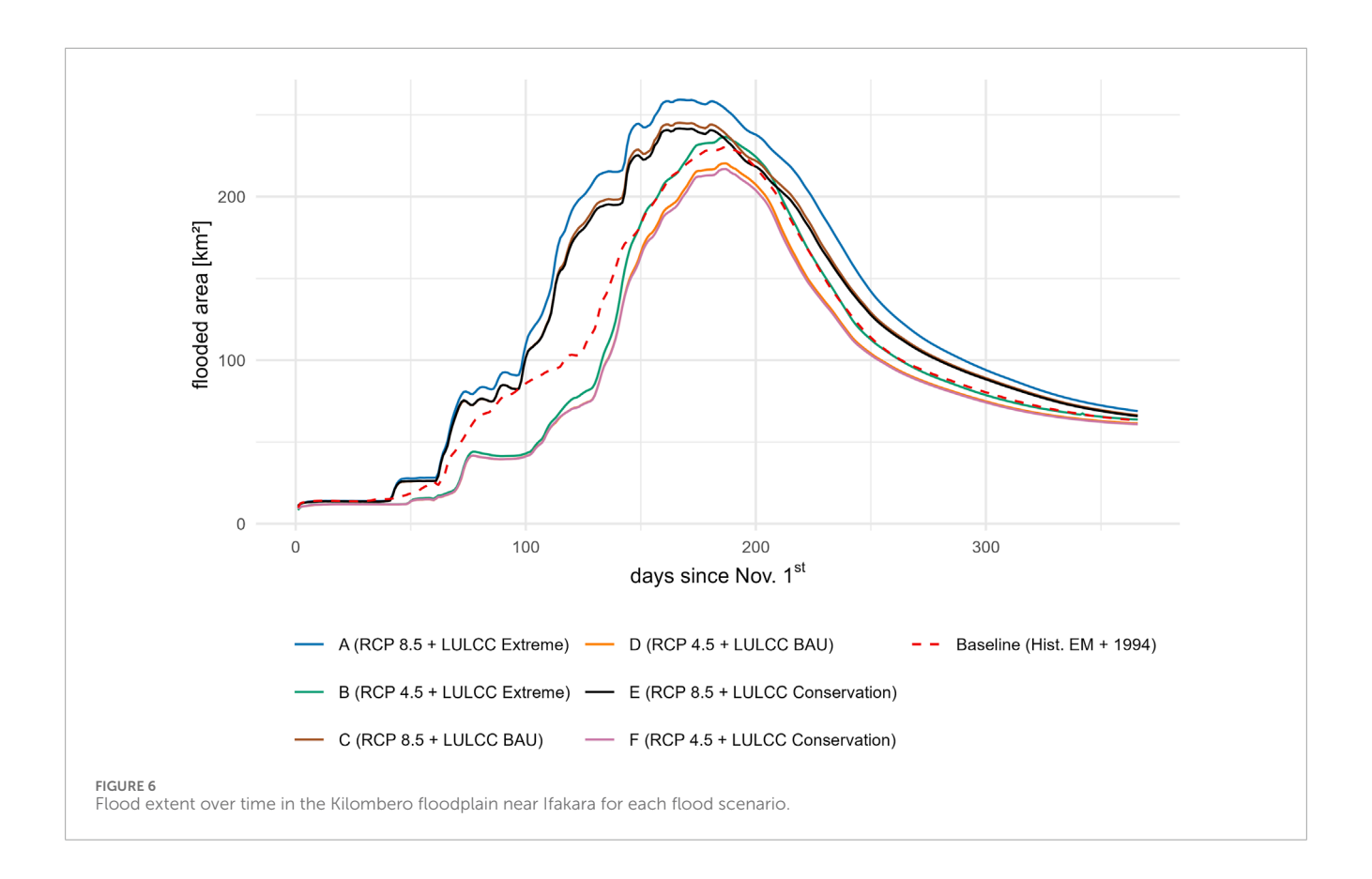
A comparison of baseline scenarios (Base1-Base6) with future scenarios (A1-F6) reveals that RCP 8.5 climate inputs generally result in an increase in the area susceptible to prolonged rice crop submergence compared to baseline conditions in most scenario combinations (see Figure 8). Only when short rice varieties (100 cm) are used in the baseline and tall varieties (130 cm) are used in RCP 8.5 scenarios, a decrease in susceptibility can be observed. However, the combination of RCP 8.5 with LULCC Extreme consistently results in increased susceptibility to submergence.

Overall, the influence of LULCC follows a clear pattern: susceptibility increases from LULCC Conservation to LULCC BAU and is highest under LULCC Extreme. Scenarios with RCP 4.5 and LULCC Extreme inputs (B-scenarios) also show increased susceptibility compared to baseline conditions in most cases. For B-scenarios, a decrease is only observed when comparing short-variety baseline scenarios with tall-variety future scenarios.

Other RCP 4.5-based scenarios (D and F) tend to show reduced susceptibility when rice varieties are either short-growing in both the baseline and future scenarios, tall-growing in both, or short-growing in the baseline and tall-growing in the future scenarios.

In contrast, future scenarios with RCP 4.5 combined with short-growing rice varieties, when compared to baseline scenarios with tall varieties, always result in increased submergence susceptibility. Generally, any comparison in which the baseline scenario uses tall varieties and the future scenario uses short ones shows an increase in susceptible area.

A comparison between scenarios with an RCP 4.5 input signal (B, D, F) in combination with short rice varieties (1-3) and



baseline scenarios in combination with tall rice varieties (4–6) consistently shows an increase in area susceptible to prolonged crop submergence. Generally, when comparing baseline scenarios with tall rice varieties to future scenarios with short rice varieties, there is always an increase in the susceptible area.

The analysis reveals that the size of the area susceptible to prolonged rice crop submergence is influenced to varying degrees by different input parameters. The Feature Importance results from the RF regression model ($R^2 = 0.939$, RMSE = 3.907) indicate that rice growth height is the dominant factor in controlling the susceptibility of rice crops to submergence in the Kilombero floodplain (see Figure 9). Discharge, which includes the climate change input signal in the hydrodynamic model, is the second most important predictor of future rice crop submergence susceptibility in the study area. The importance of LULCC falls off substantially compared to rice growth height and discharge. Submergence tolerance shows negligible influence.

4 Discussion

4.1 Modelling flood dynamics in the Kilombero floodplain using HEC-RAS 2D

This study examines potential future developments of seasonal flood dynamics in the Kilombero floodplain under various land use and climate change scenarios, in comparison to baseline conditions. We developed and validated an overall well-performing HEC-RAS 2D hydrodynamic model of the Kilombero floodplain near Ifakara,

effectively connecting catchment-scale hydrological modelling with floodplain-scale flood dynamics. Coupling hydrological and hydrodynamic modelling proved to be an efficient way to handle data scarcity regarding gauged discharge data and to enable simulations of possible future developments in the study area. This finding is consistent with studies in data-scarce regions in Africa that use a similar approach (Kleynhans et al., 2007; Chomba et al., 2021). Ultimately, coupled hydrological-hydrodynamic models can improve decision-making and planning for adaptation and mitigation measures in African floodplains (Chomba et al., 2021).

Still, the lack of measured discharge and water level data in the data-scarce Kilombero Valley hindered a more accurate validation of the model outputs, especially when considering temporally variable model outputs. In the satellite data, artefacts introduced through clouds and cloud shadows, as well as the Landsat 7 scan line corrector failure posed a challenge to quantitative validation (Storey et al., 2005). Nevertheless, the coverage with valid data was highest in the flood-affected areas of the floodplain, whereas significant gaps were primarily located in areas unlikely to experience flooding. The revisit times of 16 days of both satellites need to be considered as a factor of uncertainty in terms of the exact timing of maximum flooding. A delay between the satellite image acquisition of the assumed maximum flood extent and the modelled maximum extent limits the accuracy (Afzal et al., 2022).

Overall, discharge input and Manning's n roughness coefficient, linked to LULCC input, emerged as the primary sources of model uncertainty due to their high sensitivity, which is in line with the literature (Alipour et al., 2022). Therefore, hydrological and surface roughness input values must be carefully selected. As the discharge



FIGURE 7
Areas indicating susceptibility of rice crops to prolonged submergence per scenario (in red) in the Kilombero floodplain near Ifakara. Scenario combination (flood scenario A-F and rice scenario 1–6) in the top left corner. The size of the area susceptible to prolonged rice crop submergence is in the bottom right corner.

A (RCP 8.5, Extreme)		39.1	40	43.2	67.7	68.6	71.6
B (RCP 4.5, Extreme)	Ë,	7.5	8.3	11.5	36	36.9	39.9
C (RCP 8.5, BAU)	(100 cm, 7 days)	16.6	17.5	20.7	45.2	46.1	49.1
D (RCP 4.5, BAU)	00 da	-10.9	-10	-6.8	17.7	18.6	21.6
E (RCP 8.5, Conservation)	~ ~	12.3	13.2	16.4	40.9	41.8	44.8
F (RCP 4.5, Conservation)	~	-13.6	-12.7	-9.5	15	15.9	18.9
A (RCP 8.5, Extreme)		37.4	38.3	41.4	65.9	66.8	69.8
B (RCP 4.5, Extreme)	E, C	6.2	7.1	10.3	34.8	35.7	38.6
C (RCP 8.5, BAU)	2 (100 cm, 14 days)	14.8	15.6	18.8	43.3	44.2	47.2
D (RCP 4.5, BAU)	9 9	-11.8	-11	-7.8	16.7	17.6	20.6
E (RCP 8.5, Conservation)	~ 4	10.5	11.4	14.6	39.1	40	42.9
F (RCP 4.5, Conservation)	(4	-14.5	-13.6	-10.4	14.1	15	18
A (RCP 8.5, Extreme)		35.5	36.4	39.6	64.1	65	68
B (RCP 4.5, Extreme)	Ĕ.	2.5	3.4	6.6	31.1	32	35
C (DCD 0 5 DAII)	cr ays	13.2	14	17.2	41.7	42.6	45.6
☐ D (RCP 4.5, BAU)	90 g	-14.7	-13.8	-10.6	13.9	14.8	17.8
E (RCP 8.5, Conservation)	3 (100 cm, 21 days)	9	9.8	13	37.5	38.4	41.4
D (RCP 4.5, BAU) E (RCP 8.5, Conservation) F (RCP 4.5, Conservation)	(1)	-17.2	-16.3	-13.1	11.4	12.3	15.3
		5.4	6.3	9.4	33.9	34.8	37.8
A (RCP 8.5, Extreme) B (RCP 4.5, Extreme) C (RCP 8.5, BAU)	Ĺ.,	-24.4	-23.5	-20.3	4.2	5.1	8
5 C (RCP 8.5, BAU)	cd (S)	-14.2	-13.3	-10.1	14.4	15.3	18.3
D (RCP 4.5, BAU)	(130 cm, 7 days)	-38.9	-38	-34.8	-10.3	-9.4	-6.5
E (RCP 8.5, Conservation)	7	-17.6	-16.7	-13.5	11	11.9	14.9
F (RCP 4.5, Conservation)	4	-41.5	-40.6	-37.4	-12.9	-12	-9
A (RCP 8.5, Extreme)		3.4	4.3	7.5	32	32.9	35.9
B (RCP 4.5, Extreme)	Ë,	-25.3	-24.4	-21.3	3.2	4.1	7.1
C (RCP 8.5, BAU)	cr ays	-15.8	-14.9	-11.7	12.8	13.7	16.7
D (RCP 4.5, BAU)	30 de	-39.9	-39	-35.8	-11.3	-10.4	-7.4
E (RCP 8.5, Conservation)	5 (130 cm, 14 days)	-19.3	-18.4	-15.2	9.3	10.2	13.2
F (RCP 4.5, Conservation)	d)	-42.4	-41.5	-38.3	-13.8	-12.9	-9.9
A (RCP 8.5, Extreme)		1.5	2.4	5.6	30.1	31	34
B (RCP 4.5, Extreme)	Ë,	-28.2	-27.3	-24.1	0.4	1.3	4.3
C (RCP 8.5, BAU)	ays	-17.4	-16.5	-13.3	11.2	12.1	15
D (RCP 4.5, BAU)	6 (130 cm, 21 days)	-42.7	-41.8	-38.6	-14.1	-13.2	-10.2
E (RCP 8.5, Conservation)	21	-20.7	-19.8	-16.6	7.9	8.8	11.8
F (RCP 4.5, Conservation)	•	-44.9	-44	-40.8	-16.3	-15.4	-12.4
		1 (100 cm, 7 days)	2 (100 cm, 14 days)	3 (100 cm, 21 days)	4 (130 cm, 7 days)	5 (130 cm, 14 days)	6 (130 cm, 21 days)
		Base	Base	Base	Base	Base	Base
		(EM	(EM	(EM	(EM	(EM	(EM
		1958-2005,	1958-2005,	1958-2005,	1958-2005,	1958-2005,	1958-2005,
		1994)	1994)	1994)	1994)	1994)	1994)
				Baseline	Scenario		
		Abs	olute Chang	e from Base	line [km²]	-40 0 40)

FIGURE 8

Absolute change in susceptible area size: Future vs. Baseline Scenarios. Numbers in cells indicate absolute change (km²) between baseline scenarios (bottom) and future scenarios (left). Each future flood scenario (A-F), climate change and LULCC input signals in brackets) was combined with each of the rice scenarios (1-6, maximum growth height and temporal tolerance to submergence in brackets). The baseline flood scenario (EM = Ensemble Mean, 1958–2005 period, 1994 LULC) was combined with rice scenarios 1-6 to facilitate cross-comparison.

data was derived from the hydrological SWAT model, it can be assumed that uncertainties already inherent to the SWAT model were propagated to the hydrodynamic model outputs. Although the SWAT model performed well in the Kilombero catchment (NSE = 0.80-085, KGE = 0.89-0.93), its calibration and validation indicated that the predicted flows (95% prediction uncertainty band) encompassed 62%–67% of observed flows, with a relative width

(R-factor) of 0.45–0.56 (Näschen et al., 2018). This indicates that simulated discharges may vary within this range due to parameter and input data uncertainties, which, in turn, propagate through the HEC-RAS model. We addressed uncertainties introduced by input data by adopting a scenario-based approach that covers increasing (RCP 8.5 with wettest available GCM-RCM combination) and decreasing (RCP 4.5 with driest available GCM-RCM combination)

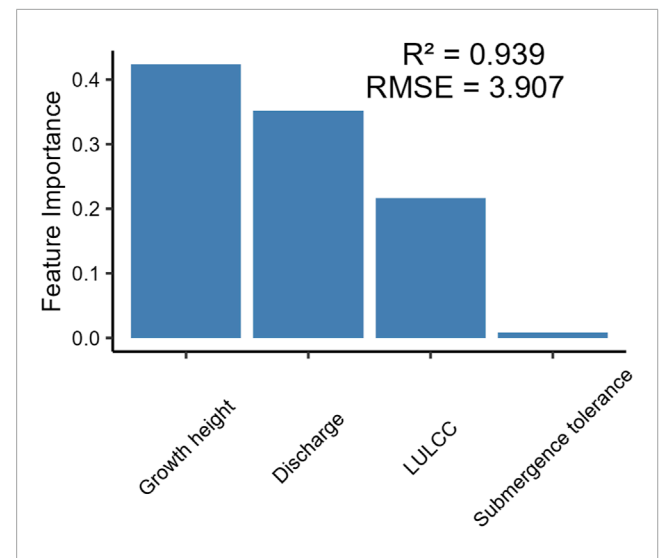


FIGURE 9
Feature Importance (mean decrease in impurity) of susceptibility input parameters calculated with RF regression model. Growth height refers to the mature growth height of rice plants. Discharge is the discharge hydrograph input in the hydrodynamic model, which includes the climate change signal. LULCC is the Land Use and Land Cover Change input (surface roughness) in the hydrodynamic model. Submergence tolerance refers to the temporal tolerance of rice plants to submergence.

annual precipitation amounts in the catchment (Näschen et al., 2019b). However, the results should be interpreted with awareness that these uncertainties affect the magnitude and timing of simulated flood peaks and flood extents.

While our scenario-based approach captures potential long-term trends in flood dynamics under RCP 4.5 and RCP 8.5, it should be noted that these deterministic pathways mainly represent mean climatic responses to radiative forcing and do not explicitly account for climate variability. Recent studies have shown that both increases and decreases in flood magnitude and frequency can be attributed to uncertainty introduced by climatic variability rather than directional change (Gao et al., 2020; Faghih and Brissette, 2023). Consequently, the RCP-based projections applied in this study represent two plausible trajectories within a wider spectrum of potential futures. Incorporating stochastic (Jafarzadegan et al., 2021) or ensemble-based (Callaghan and Hughes, 2022) frameworks in future work could therefore complement our deterministic scenarios by explicitly addressing the variability component of flood behaviour in the Kilombero floodplain.

Research indicates that rice cropping will increase in the Kilombero floodplain and move closer to the river due to increasing competition for arable land and water resources (Nindi et al., 2014; Leemhuis et al., 2017; Daconto et al., 2018; Höllermann et al., 2021; Proswitz et al., 2021). This development was addressed by implementing three LULCC scenarios (Extreme, BAU, Conservation), which project conversion from natural vegetation to rice cropland on different levels of extensiveness in the hydrodynamic model. This approach enabled the quantification of the effects of possible future LULCC scenarios on flood characteristics in the study area. The procedure

and outcome are also consistent with the existing literature (Zia et al., 2016; Jayapadma et al., 2022).

Notably, discharge at the lower boundary of the HEC-RAS 2D model does not change substantially when perturbing Manning's n in the sensitivity analysis. Still, it did affect flood depths within the floodplain. Changes in the timing and magnitude of the hydrograph become more visible with a 100% increase from base values. This behaviour could be caused by the size and low inclination of the floodplain as well as the characteristics of the hydrograph. Together, these characteristics lead to a long-lasting, shallow and extensive flooding of the floodplain, in which the effects of surface roughness are less pronounced. The limited influence of floodplain roughness on hydrograph propagation and downstream discharge in the HEC-RAS 2D model is consistent with previous findings. (Liu et al., 2019). Further uncertainty might be introduced by the resolution of the underlying DEM. However, a corrected DEM with a spatial resolution of 30 m can be considered sufficient for floodplain-scale hydrodynamic modelling, as demonstrated in previous studies (Arash and Yasi, 2023).

The results from the HEC-RAS 2D hydrodynamic model show that the climate change signal (in the discharge data) is the dominant driver of future flood dynamics in the Kilombero floodplain. The overall trend-decrease or increase in maximum flood depth and extent compared to baseline conditions-can be attributed to the climate change input signal. The results reflect the underlying hydrographs and climate change scenarios, which predict wetter conditions and an earlier peak discharge under the high-emission scenario RCP 8.5, and drier conditions under the moderate-emission scenario RCP 4.5, compared to the baseline scenario. These hydrographs were derived from the catchmentscale SWAT simulations by Näschen et al. (2019a), enabling us to translate catchment-scale hydrological projections into detailed floodplain-scale hydrodynamics and thereby link large-scale climate and LULCC impacts to local flooding processes. Contextualising these findings with similar studies in East Africa proves difficult, as the impacts of climate change are projected to be considerably heterogeneous across East Africa (Choi et al., 2022).

However, the overall trend in the results is broken by scenario B, where an RCP 4.5 climate change signal is combined with a LULCC Extreme input signal. In this scenario, discharge is lower than in the baseline, but maximum flood depths and extent are higher. The LULCC Extreme input signal stands out in particular because it shows a disproportionate change in land use towards rice in the floodplain compared to the other two LULCC input signals. LULCC Extreme shows 55.3% of land use in the model domain as rice, while LULCC BAU has 37.4% and LULCC Conservation has 29.3% rice land use (Table 3). With the applied set of Manning's n roughness coefficients, LULCC towards rice cultivation leads to increased floodplain roughness because monoculture rice plantations have a higher roughness coefficient (0.083) than grassland (0.035), which would be the natural vegetation. In turn, this leads to more extensive and deeper floods due to backwater effects (Kiss et al., 2019). In general, translating LULC data into surface roughness coefficients is considered a source of uncertainty in hydrodynamic modelling. Uncertainty can be introduced, for example, by seasonal variations in vegetation growth (e.g., rice growth stage) that are complex to reproduce (Gabriel, 2009; Ji, 2017) and model insensitivity to changes in surface roughness

(Liu et al., 2019). Potential feedback on the hydrodynamic model behaviour from different rice plant sizes, which are considered in the second step of our analysis, is also not taken into account. Simplifications further limit the HEC-RAS 2D model used in this study, as infiltration is not represented in the model. However, infiltration can be neglected as the floodplain is already saturated with rainwater and groundwater inflow from the mountains before overbank flow occurs. Consequently, floodwater infiltration does not significantly contribute to groundwater recharge in the Kilombero floodplain (Burghof et al., 2018).

4.2 Impact of global change on rice submergence susceptibility and implications for rice cultivation in the Kilombero floodplain

This study investigated the occurrence of prolonged rice crop submergence in the Kilombero floodplain under both historical and future climate and land use conditions. By integrating climate change and LULCC scenarios as well as physiological traits of rice plants in our analysis, we were able to assess spatial susceptibility patterns and derive practical implications for rice cultivation in the Kilombero floodplain. Our results demonstrate that high-emission RCP 8.5 scenarios result in larger areas susceptible to prolonged submergence of rice crops in the Kilombero floodplain compared to baseline and moderate-emission RCP 4.5 scenarios in most cases, regardless of LULCC scenario. This can be attributed to higher peak discharges and a more pronounced seasonal flood in RCP 8.5 scenarios. The results confirm findings from existing literature, suggesting that higher flood magnitudes increase the susceptibility to rice crop submergence in the Kilombero floodplain (Kwesiga et al., 2020; Grotelüschen, 2021). However, this study adds that LULCC and agricultural management decisions, such as rice variety selection (mature growth height and temporal tolerance to submergence), also control susceptibility to crop submergence. Hydrological conditions and flood characteristics are key drivers of the susceptibility of rice crops to prolonged submergence in the Kilombero floodplain. These flood characteristics are further shaped by land use in the floodplain. Recent studies in the Kilombero Valley have documented extensive conversion of grassland, savanna, and open woodland into agricultural land, particularly rice fields, and a progressive expansion of cultivation toward the main river channel and its tributaries (Thonfeld et al., 2020a; Thonfeld et al., 2020b). This spatial shift has effectively reduced the distance between anthropogenic land use and flood zones, thereby increasing the exposure of agricultural areas to flooding. Similar patterns of human encroachment toward rivers have been observed in Africa over recent decades, contributing to higher flood risk through intensified land use pressure in floodplains (Wang et al., 2023). In RCP 8.5 scenarios, land use policy could only control the rate of increase in submergence susceptibility, but it cannot prevent it. In contrast, scenarios with an RCP 4.5 input signal offer potential for mitigating risk, particularly under LULCC Conservation and LULCC BAU conditions. Well-enforced floodplain protection against land use change, particularly towards increased rice cultivation, can therefore be seen as an adaptation measure to climate change, especially under a moderate-emission climate change scenario, such as RCP 4.5. On the other hand, extensive land use change (LULCC Extreme) towards rice cultivation can increase risks for rice cultivation in the floodplain compared to LULCC BAU, LULCC Conservation, and baseline conditions, even in RCP 4.5 scenarios, as higher surface roughness leads to an increase in the depth and extent of the seasonal flood. Strengthening the enforcement of existing protection frameworks, such as the Ramsar Convention, is therefore critical for sustaining the ecological and agricultural functions of the Kilombero floodplain. Thonfeld et al. (2020a) demonstrated that almost half of the Kilombero Ramsar site is already under anthropogenic land use and that two-thirds of the land environmentally suitable for future expansion lies within protected areas. These findings underline that formal designation alone is insufficient. Effective management and enforcement are needed to balance agricultural development with wetland conservation. Moreover, effective floodplain management should also consider areas outside the current protection zones that are susceptible to future land conversion but are essential to maintaining the floodplain's hydrological and ecological integrity.

In terms of rice plant traits, taller plants with greater submergence tolerance can generally be associated with smaller areas susceptible to prolonged rice crop submergence than shorter plants with lower submergence tolerance. In fact, plant height emerged as the dominant factor in controlling crop submergence susceptibility in the Feature Importance analysis. Simulation results show that using taller plants (130 cm) instead of shorter plants (100 cm) can reduce the area susceptible to prolonged crop submergence in the Kilombero floodplain by ca. 19.7% on average. This underlines the necessity of considering rice plant height when selecting flood-resilient rice varieties for the floodplain. Moreover, taller local varieties, such as Supa India (130 cm), appear better suited to mitigate the effects of more pronounced flood events, especially under high-emission scenario RCP 8.5. Conversely, shorter, high-yielding varieties, such as Saro 5 (100 cm), which is already partially cultivated in the Kilombero floodplain, appear less adapted from this perspective. Currently, local farmers in floodprone riparian zones already favour taller varieties, suggesting an existing adaptation strategy that aligns with our findings (Michael et al., 2023a). However, it is worth noting that these traditional, taller varieties tend to produce lower yields compared to improved, shorter cultivars, such as Saro 5 (Michael et al., 2023a). Especially in the transition zone between the riparian zone and the fringe of the floodplain, where fields are not flooded every year due to interannual variability (Michael et al., 2023b), the selection of rice varieties currently is a trade-off between flood resilience and yield.

Temporal submergence tolerance of rice plants played a minor role in our analysis, as susceptibility was defined jointly by depth and duration thresholds. As flood duration is strongly correlated with flood depth, pixels experiencing deeper flooding also tend to remain flooded for longer periods. Consequently, plant height, which determines the depth threshold for complete submergence, was identified as the dominant factor in the Feature Importance analysis. However, other factors, such as floodwater quality, also affect rice submergence tolerance but were not considered in this study (Oladosu et al., 2020). Furthermore, an assessment of susceptibility to prolonged submergence in the submergence-sensitive early reproductive growth stage of rice plants was not considered and should be the subject of further research (Kwesiga et al., 2020).

The interannually varying onset and magnitude of floods still pose a challenge for establishing planting times and crop selection (Michael et al., 2023a; Michael et al., 2023b). Strategies of farmers to mitigate risks due to interannual flood variability include careful observation of weather patterns at the onset of the rainy season to inform cropping calendars and crop selection (Höllermann et al., 2021), as well as transplanting or seeding during the rainy season to maximise the use of available water. Nevertheless, transplanting or seeding during the rainy season comes with the risk of crop loss due to submergence (Kirimi et al., 2018). Our results provide practical guidance for policymakers and agricultural practitioners in the Kilombero floodplain by linking the impacts of climate and land use change on flood dynamics and agricultural management decisions.

In perspective, such a model could support adaptive planning by forecasting likely spatio-temporal flood conditions in the floodplain based on observed rainfall at the onset of the rainy season. This scenario-based approach could inform optimal rice variety selection, planting locations, and cropping calendars, particularly in the transition zone between the riparian zone and the fringe of the floodplain. Future research could extend the approach to longterm simulations that explicitly account for interannual variability. Coupling hydrodynamic flood modelling with crop-growth models would enable a more comprehensive assessment of the impacts of climate variability on rice cultivation and resilience in the Kilombero floodplain. Overall, we presented a novel approach to assess the susceptibility of rice crops to prolonged submergence in the Kilombero floodplain. East African floodplain wetlands are considered vital for the region's food security (Sakané et al., 2011; Behn et al., 2018; Gabiri et al., 2018). Our approach can contribute to a better understanding and management of humanflood interactions in terms of climate and land use change, as well as the risk and chance of specific rice cultivation techniques in East African floodplain wetlands.

5 Conclusion

This study presents a novel scenario-based approach to assessing the susceptibility of rice crops to prolonged submergence in the Kilombero floodplain under combined climate change and Land Use and Land Cover Change scenarios. By coupling hydrological and hydrodynamic modelling with physiological traits of rice plants, we identified spatial patterns of susceptibility to prolonged submergence and their primary drivers.

The study shows that climate change is a large-scale driver of flood magnitudes and prolonged crop submergence that determines the broader boundary conditions for flood risk and agricultural planning in the Kilombero floodplain but cannot be directly managed at the local level. In contrast, local management decisions, such as land use planning, enforcement of floodplain protection (e.g., Ramsar site), and the selection of suitable rice varieties, offer levers for adaptation. Especially the use of taller, submergence-tolerant rice varieties and the restriction of further agricultural expansion into active flood zones could substantially reduce the area of rice crops susceptible to prolonged submergence.

Future research should include *in situ* discharge gauging campaigns or ground-truthing of the spatiotemporal characteristics

of floods in the Kilombero floodplain to aid model calibration and validation. Furthermore, the possibilities of the coupled hydrological-hydrodynamic model for flood forecasting should be further explored to enhance cropping calendars and rice variety selection.

The findings of this study underline the value of integrating coupled hydrological-hydrodynamic modelling with crop characteristics to support adaptive agricultural planning. The developed approach can provide practical guidance for managing human-flood interactions and optimising rice cultivation in East African wetlands. It supports informed decision-making on crop variety selection for resilient agriculture in the face of global change.

Data availability statement

The raw data supporting the conclusions of this article will be made available by the authors, without undue reservation.

Author contributions

MT: Conceptualization, Data curation, Formal Analysis, Investigation, Methodology, Software, Validation, Visualization, Writing – original draft, Writing – review and editing. SS: Formal Analysis, Methodology, Validation, Writing – original draft, Writing – review and editing. HS: Formal Analysis, Methodology, Writing – review and editing. ME: Conceptualization, Supervision, Writing – review and editing.

Funding

The authors declare that financial support was received for the research and/or publication of this article. This work was supported by the Open Access Publication Fund of the University of Bonn.

Acknowledgements

We want to thank Kristian Näschen and Katharina Proswitz for providing much of the underlying data for this study.

Conflict of interest

The authors declare that the research was conducted in the absence of any commercial or financial relationships that could be construed as a potential conflict of interest.

Generative AI statement

The authors declare that no Generative AI was used in the creation of this manuscript.

Any alternative text (alt text) provided alongside figures in this article has been generated by Frontiers with the support of

artificial intelligence and reasonable efforts have been made to ensure accuracy, including review by the authors wherever possible. If you identify any issues, please contact us. reviewers. Any product that may be evaluated in this article, or claim that may be made by its manufacturer, is not guaranteed or endorsed by the publisher.

Publisher's note

All claims expressed in this article are solely those of the authors and do not necessarily represent those of their affiliated organizations, or those of the publisher, the editors and the

Supplementary material

The Supplementary Material for this article can be found online at: https://www.frontiersin.org/articles/10.3389/feart.2025.1672749/full#supplementary-material

References

Afzal, M. A., Ali, S., Nazeer, A., Khan, M. I., Waqas, M. M., Aslam, R. A., et al. (2022). Flood inundation modeling by integrating HEC–RAS and satellite imagery: a case study of the Indus River Basin. *Water* 14 (19), 2984. doi:10.3390/w14192984

Airbus (2022). Copernicus DEM. Product handbook. Available online at: https://dataspace.copernicus.eu/sites/default/files/media/files/2024-06/geo1988-copernicusdem-spe-002_producthandbook_i5.0.pdf (Accessed January 16, 2025).

Alawadi, W. A., Al-Tofan, M., Al-Suraifi, A., and Al-Rekabi, W. S. (2023). 2D hydraulic modeling for predicting water depth and velocity changes in Al Hawizeh wetland in response to dry conditions. *Model. Earth Syst. Environ.* 9 (1), 631–646. doi:10.1007/s40808-022-01524-1

Alipour, A., Jafarzadegan, K., and Moradkhani, H. (2022). Global sensitivity analysis in hydrodynamic modeling and flood inundation mapping. *Environ. Model. and Softw.* 152, 105398. doi:10.1016/j.envsoft.2022.105398

Almazroui, M., Saeed, F., Saeed, S., Nazrul Islam, M., Ismail, M., Klutse, N. A. B., et al. (2020). Projected change in temperature and precipitation over Africa from CMIP6. *Earth Syst. Environ.* 4 (3), 455–475. doi:10.1007/s41748-020-00161-x

Arash, A. M., and Yasi, M. (2023). The assessment for selection and correction of RS -based DEMs and 1D and 2D HEC-RAS models for flood mapping in different river types. *J. Flood Risk Manag.* 16 (1), e12871. doi:10.1111/jfr3.12871

Ayyad, S., Karimi, P., Langensiepen, M., Ribbe, L., Rebelo, L.-M., and Becker, M. (2022). Remote sensing assessment of available green water to increase crop production in seasonal floodplain wetlands of Sub-Saharan Africa. *Agric. Water Manag.* 269, 107712. doi:10.1016/j.agwat.2022.107712

Behn, K., Becker, M., Burghof, S., Möseler, B. M., Willy, D. K., and Alvarez, M. (2018). Using vegetation attributes to rapidly assess degradation of East African wetlands. *Ecol. Indic.* 89, 250–259. doi:10.1016/j.ecolind.2018.02.017

Brunner, G. W. (2021). HEC-RAS River Analysis System: user's Manual Version 6.0. Davis, CA: U.S. Army Corps of Engineers, Institute for Water Resources. Available online at: https://www.hec.usace.army.mil/software/hec-ras/documentation/HEC-RAS_6.0_UsersManual.pdf (Accessed February 12, 2025).

Burghof, S. (2017). Hydrogeology and water quality of wetlands in East Africa: case studies of a floodplain and a valley bottom wetland. Bonn: University of Bonn.

Burghof, S., Gabiri, G., Stumpp, C., Chesnaux, R., and Reichert, B. (2018). Development of a hydrogeological conceptual wetland model in the data-scarce north-eastern region of kilombero valley, Tanzania. *Hydrogeol. J.* 26 (1), 267–284. doi:10.1007/s10040-017-1649-2

Callaghan, D. P., and Hughes, M. G. (2022). Assessing flood hazard changes using climate model forcing. *Nat. Hazards Earth Syst. Sci.* 22 (8), 2459–2472. doi:10.5194/nhess-22-2459-2022

Cappelli, F., and Grimaldi, S. (2023). Feature importance measures for hydrological applications: insights from a virtual experiment. *Stoch. Environ. Res. Risk Assess.* 37 (12), 4921–4939. doi:10.1007/s00477-023-02545-7

Choi, Y.-W., Campbell, D. J., and Eltahir, E. A. (2022). Near-term regional climate change in East Africa. *Clim. Dyn.* 61, 961–978. doi:10.1007/s00382-022-06591-9

Chomba, I. C., Banda, K. E., Winsemius, H. C., Chomba, M. J., Mataa, M., Ngwenya, V., et al. (2021). A review of coupled hydrologic-hydraulic models for floodplain assessments in Africa: opportunities and challenges for floodplain wetland management. *Hydrology* 8 (1), 44. doi:10.3390/hydrology8010044

Collins, M., Knutti, R., Arblaster, J., Dufresne, J.-L., Fichefet, T., Friedlingstein, P., et al. (2013). "Long-term climate change: projections, commitments and irreversibility," in Climate change 2013: the physical science basis. Contribution of working group 1 to the fifth assessment report of the intergovernmental panel on climate change (Cambridge University Press), 1029–1136.

Corcoran, J., Knight, J., Pelletier, K., Rampi, L., and Wang, Y. (2015). The effects of point or polygon based training data on RandomForest classification accuracy of wetlands. *Remote Sens.* 7 (4), 4002–4025. doi:10.3390/rs70404002

Daconto, G., Games, I., Lukumbuzya, K., and Raijmakers, F. (2018). Integrated management plan for the kilombero valley ramsar site.

Desalegn, H., and Mulu, A. (2021). Mapping flood inundation areas using GIS and HEC-RAS model at fetam river, upper abbay basin, Ethiopia. *Sci. Afr.* 12, e00834. doi:10.1016/j.sciaf.2021.e00834

Dixon, A. B., and Wood, A. P. (2003). Wetland cultivation and hydrological management in eastern Africa: matching community and hydrological needs through sustainable wetland use. *Nat. Resour. Forum* 27 (2), 117–129. doi:10.1111/1477-8947.00047

Emery, C. M., Larnier, K., Liquet, M., Hemptinne, J., Vincent, A., and Peña Luque, S. (2021). Extraction of roughness parameters from remotely-sensed products for hydrology applications. doi:10.5194/hess-2021-551

ESA (2025). Copernicus DEM – global and European digital elevation model. Available online at: https://dataspace.copernicus.eu/explore-data/data-collections/copernicus-contributing-missions/collections-description/COP-DEM (Accessed January 16, 2025).

Faghih, M., and Brissette, F. (2023). The role of internal climate variability on future streamflow projections. *J. Hydrology* 625, 130101. doi:10.1016/j.jhydrol.2023. 130101

Gabiri, G., Burghof, S., Diekkrüger, B., Leemhuis, C., Steinbach, S., and Näschen, K. (2018). Modeling spatial soil water dynamics in a tropical floodplain, East Africa. *Water* 10 (2), 191. doi:10.3390/w10020191

Gabiri, G., Leemhuis, C., Diekkrüger, B., Näschen, K., Steinbach, S., and Thonfeld, F. (2019). Modelling the impact of land use management on water resources in a tropical inland valley catchment of central Uganda, East Africa. *Sci. total Environ.* 653, 1052–1066. doi:10.1016/j.scitotenv.2018.10.430

Gabiri, G., Diekkrüger, B., Näschen, K., Leemhuis, C., van der Linden, R., Majaliwa, J.-G. M., et al. (2020). Impact of climate and land Use/Land cover change on the water resources of a tropical inland Valley catchment in Uganda, East Africa. *Climate* 8 (7), 83. doi:10.3390/cli8070083

Gabriel, H. (2009). Hydrodynamische Modellierung von Oberflächengewässern. Österr. Wasser- Abfallw 61 (7-8), 99–104. doi:10.1007/s00506-009-0099-z

Gao, C., Booij, M. J., and Xu, Y.-P. (2020). Assessment of extreme flows and uncertainty under climate change: disentangling the uncertainty contribution of representative concentration pathways, global climate models and internal climate variability. *Hydrology Earth Syst. Sci.* 24 (6), 3251–3269. doi:10.5194/hess-24-3251-2020

Gebrekidan, B. H., Heckelei, T., and Rasch, S. (2020). Characterizing farmers and farming System in Kilombero Valley floodplain, Tanzania. *Sustainability* 12 (17), 7114. doi:10.3390/su12177114

Grotelüschen, K. (2021). Evaluating rice performance in contrasting East African wetlands using an experimental and modelling approach. Bonn: University of Bonn.

Gxokwe, S., Dube, T., and Mazvimavi, D. (2022). Leveraging Google Earth engine platform to characterize and map small seasonal wetlands in the semi-arid environments of South Africa. *Sci. Total Environ.* 803, 150139. doi:10.1016/j.scitotenv.2021.150139

Haile, G. G., Tang, Q., Hosseini-Moghari, S.-M., Liu, X., Gebremicael, T. G., Leng, G., et al. (2020). Projected impacts of climate change on drought patterns over East Africa. *Earth's Future* 8 (7), e2020EF001502. doi:10.1029/2020EF001502

Höllermann, B., Näschen, K., Tibanyendela, N., Kwesiga, J., and Evers, M. (2021). Dynamics of human-water interactions in the Kilombero Valley, Tanzania: insights from farmers' aspirations and decisions in an uncertain environment. *Eur. J. Dev. Res.* 33 (4), 980–999. doi:10.1057/s41287-021-00390-4

Jafarzadegan, K., Abbaszadeh, P., and Moradkhani, H. (2021). Sequential data assimilation for real-time probabilistic flood inundation mapping. *Hydrology Earth Syst. Sci.* 25 (9), 4995–5011. doi:10.5194/hess-25-4995-2021

- James, R., Washington, R., and Rowell, D. P. (2013). Implications of global warming for the climate of African rainforests. *Philosophical Trans. R. Soc. Lond. Ser. B, Biol. Sci.* 368 (1625), 20120298. doi:10.1098/rstb.2012.0298
- Janssen, C. (2016). Manning's n values for various land covers to use for dam breach analyses by NRCS in Kansas. Available online at: https://rashms.com/wp-content/uploads/2021/01/Mannings-n-values-NLCD-NRCS.pdf (Accessed December 4, 2024).
- Jätzold, R., and Baum, E. (1968). "The Kilombero Valley (Tanzania) characteristic features of the economic geography of a semihumid East African flood plain and its margins," München. Weltforum-Verlag GmbH.
- Jayapadma, J. M. M. U., Wickramaarachchi, T. N., Silva, G. H. A. C., Ishidaira, H., and Magome, J. (2022). Coupled hydrodynamic modelling approach to assess land use change induced flood characteristics. *Environ. Monit. Assess.* 194 (5), 354. doi:10.1007/s10661-022-09986-7
- Ji, Z.-G. (2017). Hydrodynamics and water quality: modeling rivers, lakes, and estuaries. Hoboken, NJ: John Wiley and Sons, Inc.
- Kato, F. (2007). Development of a major rice cultivation area in the Kilombero valley, Tanzania. *Afr. Study Monogr.* (36), 3–18.
- Kirimi, F., Thiong'o, K., Gabiri, G., Diekkrüger, B., and Thonfeld, F. (2018). Assessing seasonal land cover dynamics in the tropical Kilombero floodplain of East Africa. *J. Appl. Rem. Sens.* 12 (02), 1. doi:10.1117/1.JRS.12.026027
- Kiss, T., Nagy, J., Fehérváry, I., and Vaszkó, C. (2019). (Mis) management of floodplain vegetation: the effect of invasive species on vegetation roughness and flood levels. *Sci. Total Environ.* 686, 931–945. doi:10.1016/j.scitotenv.2019.06.006
- Kitilu, M. J. F., Nyomora, A. M. S., and Charles, J. (2019). Growth and yield performance of selected upland and lowland rainfed rice varieties grown in farmers and researchers managed fields at Ifakara, Tanzania. *Afr. J. Agric. Res.* 14 (4), 197–208. doi:10.5897/AIAR2018.13611
- Kleynhans, M. T., James, C. S., and Birkhead, A. L. (2007). Hydrologic and hydraulic modelling of the Nyl River floodplain Part 3: applications to assess ecological impact. WSA 33 (1). doi:10.4314/wsa.v33i1.47867
- Koutsouris, A. J., Chen, D., and Lyon, S. W. (2016). Comparing global precipitation data sets in eastern Africa: a case study of Kilombero Valley, Tanzania. *Int. J. Climatol.* 36 (4), 2000–2014. doi:10.1002/joc.4476
- Kwesiga, J., Grotelüschen, K., Senthilkumar, K., Neuhoff, D., Döring, T. F., and Becker, M. (2020). Rice yield gaps in smallholder systems of the Kilombero floodplain in Tanzania. *Agronomy* 10 (8), 1135. doi:10.3390/agronomy10081135
- Leemhuis, C., Thonfeld, F., Näschen, K., Steinbach, S., Muro, J., Strauch, A., et al. (2017). Sustainability in the food-water-ecosystem nexus: the role of land use and land cover change for water resources and ecosystems in the Kilombero wetland, Tanzania. *Sustainability* 9 (9), 1513. doi:10.3390/su9091513
- Liu, Z., Merwade, V., and Jafarzadegan, K. (2019). Investigating the role of model structure and surface roughness in generating flood inundation extents using one- and two-dimensional hydraulic models. *J. Flood Risk Manage.* 12 (1), e12347. doi:10.1111/jfr3.12347
- Lyon, S. W., Koutsouris, A., Scheibler, F., Jarsjö, J., Mbanguka, R., Tumbo, M., et al. (2015). Interpreting characteristic drainage timescale variability across Kilombero Valley, Tanzania. *Hydrol. Process.* 29 (8), 1912–1924. doi:10.1002/hyp.10304
- McFeeters, S. K. (1996). The use of the Normalized Difference Water Index (NDWI) in the delineation of open water features. *Int. J. Remote Sens.* 17 (7), 1425-1432. doi:10.1080/01431169608948714
- Michael, P. S., Mwakyusa, L., Sanga, H. G., Shitindi, M. J., Kwaslema, D. R., Herzog, M., et al. (2023a). Floods stress in lowland rice production: experiences of rice farmers in Kilombero and Lower-Rufiji floodplains, Tanzania. *Front. Sustain. Food Syst.* 7, 1206754. doi:10.3389/fsufs.2023.1206754
- Michael, P. S., Sanga, H. G., Shitindi, M. J., Herzog, M., Meliyo, J. L., and Massawe, B. H. J. (2023b). Uncovering spatiotemporal pattern of floods with Sentinel-1 synthetic aperture radar in major rice-growing river basins of Tanzania. *Front. Earth Sci.* 11, 1183834. doi:10.3389/feart.2023.1183834
- Millard, K., and Richardson, M. (2015). On the importance of training data sample selection in random Forest image classification: a case Study in peatland ecosystem mapping. *Remote Sens.* 7 (7), 8489–8515. doi:10.3390/rs70708489
- Ming, X., Liang, Q., and Jiang, J. (2025). Large-Scale high-resolution hydrodynamic modelling of urban floods: some practical considerations. *J. Hydro-Environment Res.* 59, 100655. doi:10.1016/j.jher.2025.100655
- Mombo, F. M., Speelman, S., van Huylenbroeck, G., Hella, J., Pantaleo, M., and Moe, S. (2011). Ratification of the Ramsar convention and sustainable wetlands management: situation analysis of the Kilombero Valley wetlands in Tanzania. *J. Agric. Ext. Rural Dev.* 3 (9), 153–164.
- Mubialiwo, A., Abebe, A., Kawo, N. S., Ekolu, J., Nadarajah, S., and Onyutha, C. (2022). Hydrodynamic modelling of floods and estimating socio-economic impacts of floods in Ugandan River malaba sub-catchment. *Earth Syst. Environ.* 6 (1), 45–67. doi:10.1007/s41748-021-00283-w
- Munishi, S., and Jewitt, G. (2019). Degradation of Kilombero Valley Ramsar wetlands in Tanzania. *Phys. Chem. Earth, Parts A/B/C* 112, 216–227. doi:10.1016/j.pce.2019.03.008

- Näschen, K., Diekkrüger, B., Leemhuis, C., Steinbach, S., Seregina, L., Thonfeld, F., et al. (2018). Hydrological modeling in data-scarce catchments: the kilombero floodplain in Tanzania. *Water* 10 (5), 599. doi:10.3390/w10050599
- Näschen, K., Diekkrüger, B., Evers, M., Höllermann, B., Steinbach, S., and Thonfeld, F. (2019a). The impact of land Use/Land cover change (LULCC) on water resources in a tropical catchment in Tanzania under different climate change scenarios. *Sustainability* 11 (24), 7083. doi:10.3390/su11247083
- Näschen, K., Diekkrüger, B., Leemhuis, C., Seregina, L., and van der Linden, R. (2019b). Impact of climate change on water resources in the Kilombero catchment in Tanzania. *Water* 11 (4), 859. doi:10.3390/w11040859
- Nindi, S. J., Maliti, H., Bakari, S., Kija, H., and Machoke, M. (2014). Conflicts over land and water resources in the Kilombero Valley. *Afr. Study Monogr.* 50, 173–190.
- Notter, B., Hurni, H., Wiesmann, U., and Ngana, J. O. (2013). Evaluating watershed service availability under future management and climate change scenarios in the Pangani Basin. *Phys. Chem. Earth* 61-62, 1–11. doi:10.1016/j.pce.2012.08.017
- Oladosu, Y., Rafii, M. Y., Arolu, F., Chukwu, S. C., Muhammad, I., Kareem, I., et al. (2020). Submergence tolerance in rice: review of mechanism, breeding and, future prospects. *Sustainability* 12 (4), 1632. doi:10.3390/su12041632
- Paiva, R. C. D. de, Buarque, D. C., Collischonn, W., Bonnet, M.-P., Frappart, F., Calmant, S., et al. (2013). Large-scale hydrologic and hydrodynamic modeling of the Amazon River basin. *Water Resour. Res.* 49 (3), 1226–1243. doi:10.1002/wrcr.20067
- Panda, D., Barik, J., and Sarkar, R. K. (2021). Recent advances of genetic resources, genes and genetic approaches for flooding tolerance in rice. Curr. genomics 22 (1), 41–58. doi:10.2174/1389202922666210114104140
- Pinos, J., and Timbe, L. (2019). Performance assessment of two-dimensional hydraulic models for generation of flood inundation maps in mountain river basins. *Water Sci. Eng.* 12 (1), 11–18. doi:10.1016/j.wse.2019.03.001
- Proswitz, K., Edward, M. C., Evers, M., Mombo, F., Mpwaga, A., Näschen, K., et al. (2021). Complex Socio-Ecological systems: translating narratives into future land use and land cover scenarios in the Kilombero Catchment, Tanzania. *Sustainability* 13 (12), 6552. doi:10.3390/su13126552
- Rao, S., Surwase, T., Begum, A., Reddy, K. M., and Rao, J. (2019). 2D flood simulation and development of flood hazard map by using hydraulic model. $\it IJARSG~8~(1)$, 3096–3105. doi:10.23953/cloud.ijarsg.424
- Sakané, N., Alvarez, M., Becker, M., Böhme, B., Handa, C., Kamiri, H. W., et al. (2011). Classification, characterisation, and use of small wetlands in East Africa. *Wetlands* 31 (6), 1103–1116. doi:10.1007/s13157-011-0221-4
- Samantaray, D., Chatterjee, C., Singh, R., Gupta, P. K., and Panigrahy, S. (2015). Flood risk modeling for optimal rice planning for delta region of Mahanadi river basin in India. *Natural Hazards* 76 (1), 347–372. doi:10.1007/s11069-014-1493-9
- Shongwe, M. E., van Oldenborgh, G. J., van den Hurk, B., and van Aalst, M. (2011). Projected changes in mean and extreme precipitation in Africa under global warming. Part II: east Africa. *J. Clim.* 24 (14), 3718–3733. doi:10.1175/2010JCLI2
- Singh, S., Mackill, D. J., and Ismail, A. M. (2011). Tolerance of longer-term partial stagnant flooding is independent of the SUB1 locus in rice. *Field Crops Res.* 121 (3), 311–323. doi:10.1016/j.fcr.2010.12.021
- Singh, A., Septiningsih, E. M., Balyan, H. S., Singh, N. K., and Rai, V. (2017). Genetics, physiological mechanisms and breeding of flood-tolerant rice (Oryza sativa L.). *Plant and Cell physiology* 58 (2), 185–197. doi:10.1093/pcp/pcw206
- Singh, R. K., Kumar Villuri, V. G., Pasupuleti, S., and Nune, R. (2020). Hydrodynamic modeling for identifying flood vulnerability zones in lower Damodar river of eastern India. *Ain Shams Eng. J.* 11 (4), 1035–1046. doi:10.1016/j.asej.2020.01.011
- Storey, J. C., Scaramuzza, P. L., and Schmidt, G. L. (2005). Lands at 7 scan line corrector-off gap-filled product development.
- Thiemig, V., Bisselink, B., Pappenberger, F., and Thielen, J. (2015). A Pan-African medium-range ensemble flood forecast system. *Hydrology Earth Syst. Sci.* 19 (8), 3365–3385. doi:10.5194/hess-19-3365-2015
- Thonfeld, F., Steinbach, S., Muro, J., Hentze, K., Games, I., Näschen, K., et al. (2020a). The impact of anthropogenic land use change on the protected areas of the Kilombero catchment, Tanzania. *ISPRS J. Photogrammetry Remote Sens.* 168, 41–55. doi:10.1016/j.isprsjprs.2020.07.019
- Thonfeld, F., Steinbach, S., Muro, J., and Kirimi, F. (2020b). Long-Term land Use/Land cover change assessment of the Kilombero catchment in Tanzania using random Forest classification and robust change vector analysis. *Remote Sens.* 12 (7), 1057. doi:10.3390/rs12071057
- Timbadiya, P. V., Patel, P. L., and Porey, P. D. (2011). Calibration of HEC-RAS model on prediction of flood for lower tapi River, India. *J. Water Res. Prot.* 03 (11), 805–811. doi:10.4236/jwarp.2011.311090
- Tucker, C. J. (1979). Red and photographic infrared linear combinations for monitoring vegetation. *Remote Sens. Environ.* 8 (2), 127–150. doi:10.1016/0034-4257(79)90013-0
- United Republic of Tanzania (2004). Basic data, agriculture sector 2003/2004. Ministry Agric. Food Secur.

van der Linden, S., Rabe, A., Held, M., Jakimow, B., Leitão, P., Okujeni, A., et al. (2015). The EnMAP-Box—A toolbox and application programming interface for EnMAP data processing. *Remote Sens.* 7 (9), 11249–11266. doi:10.3390/rs70911249

Wang, N., Sun, F., Koutsoyiannis, D., Iliopoulou, T., Wang, T., Wang, H., et al. (2023). How can changes in the Human-Flood distance mitigate flood fatalities and displacements? *Geophys. Res. Lett.* 50 (20), Article e2023GL105064. doi:10.1029/2023GL105064

Wilson, E., McInnes, R., Mbaga, D. P., and Ouedaogo, P. (2017). Ramsar advisory Mission report: united Republic of Tanzania. Kilombero Valley, Gland, Switzerland.

Xu, K., Xu, X., Fukao, T., Canlas, P., Maghirang-Rodriguez, R., Heuer, S., et al. (2006). Sub1A is an ethylene-response-factor-like gene that confers submergence tolerance to rice. Nature~442~(7103),~705-708.~doi:10.1038/nature04920

Yalcin, E. (2020). Assessing the impact of topography and land cover data resolutions on two-dimensional HEC-RAS hydrodynamic model simulations for urban flood hazard analysis. Nat. Hazards 101 (3), 995–1017. doi:10.1007/s11069-020-03906-z

Yang, Q., Wu, W., Wang, Q. J., and Vaze, J. (2022). A 2D hydrodynamic model-based method for efficient flood inundation modelling. J. Hydroinformatics 24 (5), 1004–1019. doi:10.2166/hydro.2022.133

Zhu, Z., and Woodcock, C. E. (2012). Object-based cloud and cloud shadow detection in Landsat imagery. *Remote Sens. Environ.* 118, 83–94. doi:10.1016/j.rse.2011. 10.028

Zhu, Z., Wang, S., and Woodcock, C. E. (2015). Improvement and expansion of the Fmask algorithm: cloud, cloud shadow, and snow detection for Landsats 4–7, 8, and Sentinel 2 images. *Remote Sens. Environ.* 159, 269–277. doi:10.1016/j.rse.2014.

Zia, A., Bomblies, A., Schroth, A. W., Koliba, C., Isles, P. D. F., Tsai, Y., et al. (2016). Coupled impacts of climate and land use change across a river–lake continuum: insights from an integrated assessment model of Lake Champlain's Missisquoi Basin, 2000–2040. *Environ. Res. Lett.* 11 (11), 114026. doi:10.1088/1748-9326/11/11/